Polydioxythiophene Nanodots, Nonowires, Nano-Networks, and Tubular Structures: The Effect of Functional Groups and Temperature in Template-Free Electropolymerization

Shyh-Chyang Luo,* Jun Sekine, Bo Zhu, Haichao Zhao, Aiko Nakao, and Hsiao-hua Yu*

Yu Initiative Research Unit, RIKEN Advanced Science Institute, 2-1 Hirosawa, Wako, Saitama, 351-0198, Japan

ABSTRACT Various nanostructures, including nanofibers, nanodots, nanonetwork, and nano- to microsize tubes of functionalized poly(3,4-ethylenedioxythiophene) (EDOT) and poly(3,4-propylenedioxythiophene) (ProDOT) are created by using a template-free electropolymerization method on indium–tin–oxide substrates. By investigating conducting polymer nanostructures containing various functional groups prepared at different polymerization temperature, we conclude a synergistic effect of functional groups and temperature on the formation of polymer nanostructures when a template-free electropolymerization method is applied. For unfunctionalized EDOT and ProDOT, or EDOT containing alkyl functional groups, nanofibers and nanoporous structures are usually found. Interesting, when polar functional groups are attached, conducting polymers tend to form nanodots at room temperature while grow tubular structures at low temperature. The relationship between surface properties and their nanostructures is evaluated by contact angle measurements. The capacity and electrochemical impedance spectroscopy measurements were conducted to understand the electrical properties of using these materials as electrodes. The results provide the relationship between the functional groups, nanostructures, and electrical properties. We also discuss the potential restriction of using this method to create nanostructures. The copolymerization of different functionalized EDOTs may cause irregular and unexpected nanostructures, which indicates the complex interaction between different functionalized monomers during the electropolymerization.

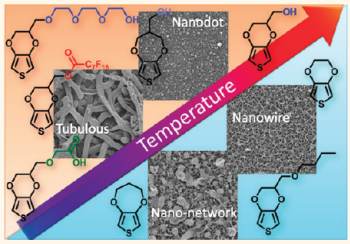

KEYWORDS: electropolymerization · conducting polymers · poly(3,4-ethylenedioxythiophene) · nanostructures · surface wettibility · cathodal charge storage capacity · electrochemical impedance spectroscopy

To synthesize various nanostructures of conducting polymers has been one of the most important research topics in this field because a nanostructure usually provides different or even superior electric or electrochemical properties compared to traditional conducting polymers.[1–3] Owing to the nanosize effect, the charge transporting rate is highly sensitive to environmental parameters, such as gas, surface chemistry, temperature, or mechanical stress.[4,5] This intrinsic property makes conducting polymer nanostructures good candidates for ultrasensitive gas and chemical sensors.[6,7] Besides, the higher surface-to-volume ratio of nanostructures also provides more efficient reactivity, which is critical in the development of highly efficient organic electronics, such as supercapacitors,[8] energy storage devices,[9] and high reactivity electrodes.[10] Most recently, people have used conducting polymers for various bioengineering applications, such as tissue engineering,[11] neuron probes,[12,13] biosensors,[14–18] and controlled drug release,[19–21] due to their superior biocompatibility and conductivity.[22–24] To make nanostructures for these applications is especially critical because many biological phenomena are at nanoscale. Until now, several methods have successfully demonstrated the manufacture of well-controlled and organized conducting polymer nanostructures.[3,25] By using oxidants for chemical polymerization, researchers have synthesized conducting polymer nanoparticles by using polystyrene beads as hard templates,[26,27] and conducting polymer nanorods by using surfactants as soft templates.[28,29] A few template-free methods have also been developed, such as using dimers for seeds during the polymerization.[2,30] By using electropolymerization, people also demonstrated conducting polymer nanowire and nanorod arrays by using anodic aluminum oxide,[31,32] block copolymers,[5] or polystyrene beads[33] as hard templates. Moreover, several studies also demonstrated the feasibility to create certain conducting polymer nanostructures by programming the electric pulse sequences[34,35] without the assistance of hard templates. Although the template-free method

* Address correspondence to scluo@riken.jp, bruceyu@riken.jp.

Received for review November 21, 2011 and accepted March 16, 2012.

Published online March 16, 2012
10.1021/nn300737e

provided a simple and straight way to create conducting polymer nanostructures directly on conductive substrates, only certain type of monomers and nanostructure were achieved by this method so far. Therefore, it is highly interesting to know the feasibility and the potential restriction of using a template-free electropolymerization method to create conducting polymer nanostructures.

In this manuscript, we would like to demonstrate our interesting findings showing how chemical structure of functional groups, temperature, and a synergistic effect of these two factors influence the formation of nanostructures when the template-free electropolymerization was performed. Functionalized 3,4-ethylenedioxythiophene (EDOT)[20,36] and 3,4-propylenedioxythiophene (ProDOT)[37] were used as our building blocks in this study due to the accessibility to various functionalizations. Until now, several functionalized EDOTs have been successfully synthesized and demonstrated.[36,37] Hydroxyl, carboxylic acid, and azide functional groups provided the bioconjugation function.[38−40] Ethylene glycol groups provided hydrophilic surfaces for preventing the nonspecific binding.[41] Alkyl and perfluorocarbon groups were used to create a superhydrophobic and self-cleaning surface.[35,42] Although some studies have demonstrated solvent[43,44] and counterion effects[45] on the formation of nanostructures of unfunctionalized PEDOT, only few studies[42,46] demonstrated the nanostructure of functional PEDOTs and discussed the relationship between their functional groups and nanostructures systematically. Therefore, we were very interested in investigating how these functional groups affect the polymer growth which leads to formation of different nanostructures. Furthermore, besides the functional group effect, we would add the temperature effect on the formation of nanostructures. Although some studies have shown that the polymerization rate and conductivity are affected by the temperature for electropolymerization,[47,48] few studies discussed the temperature effect on polymer morphology. In this study, we demonstrate that temperature also plays an important role on the formation of nanostructures. The EDOTs with certain functional groups form dramatically different nanostructures, indicating different polymer growth mechanisms when the temperature was changed. By investigating the functional group effect, temperature effect, and the synergistic effect of these two factors, we hope this study can provide some insight on the formation of polymer nanostructures during electropolymerization, and the potential restriction of using this template-free electropolymerization to create nanostructures.

RESULTS AND DISCUSSION

Since the focus of this study is to evaluate the effect of functional group and temperature, all the

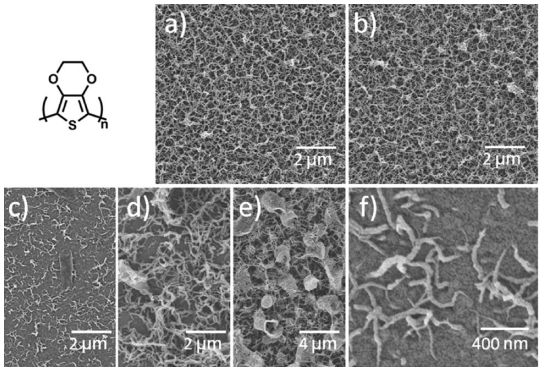

Figure 1. Scanning electron microscope images of electropolymerized PEDOT nanostructures by applying a constant voltage (*vs* Ag/Ag$^+$): (a) 1.2 V at 25 °C for 30 s; (b) 1.4 V at 25 °C for 30 s; 1.4 V at 0 °C for (c) 30 s, (d) 60 s, and (e) 90 s. (f) High magnification images of the PEDOT nanostructures in panel c.

electropolymerization was performed by applying a constant voltage method in the same solvent system (dichloromethane (CH_2Cl_2) as solvent and 100 mM tetrabutyl ammonium perchlorate (TBAP) as electrolytes). Indium−tin−oxide (ITO) coated glass was used for the conductive substrates. The electropolymerization *I*−*V* curves of all monomers used in this manuscript by applying cyclic potentials from −0.6 to 1.5 V (*vs* Ag/Ag$^+$) were provided in Supporting Information. All monomers showed steadily growth when the applied voltage was lower than 1.5 V in this solution system. First, we evaluated the PEDOT morphology prepared in this solvent system under several polymerization conditions as shown in Figure 1. Generally, PEDOT formed a nanofiber-type nanostructure when prepared from TBAP/CH_2Cl_2 solution as shown in Figure 1a. A comparison of Figure 1b to Figure 1a, shows that changing the applied voltage from 1.2 to 1.4 V (*vs* Ag/Ag$^+$) did not obviously affect PEDOT morphology, which indicates that the applied voltage is not the main factor to affect polymer morphology in this system. The PEDOT morphology prepared at 0 °C was shown in Figure 1c−f. In a comparison of Figure 1 panels b and c, the PEDOT nanofibers prepared at 0 °C were much shorter and the density was lower compared to that prepared at 25 °C, which indicates a slower polymerization rate. But PEDOT still formed nanofibers when prepared at 0 °C. As the polymerization time increased, the nanofibers grew longer and the density was higher as shown in panels d and e. Besides, some nanofibers started to aggregate and form some microstructure when the density was higher as shown in panel e. From the high magnification of SEM as shown in Figure 1f, the formation of PEDOT nanofibers was clearly observed. On the other hand, poly(EDOT−OH) nanostructures were shown in Figure 2. A comparison of Figure 2a to Figure 1a shows that instead of forming a fibril structure like PEDOT, poly(EDOT−OH) formed nanodots when electropolymerization proceeded

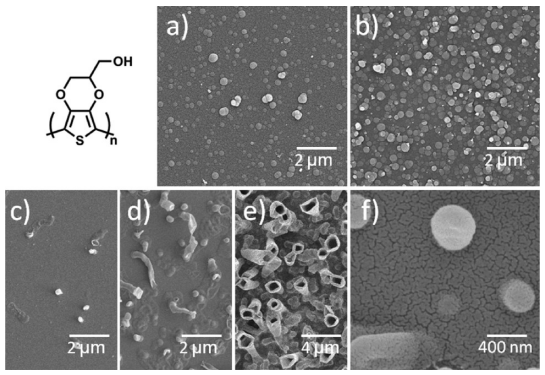

Figure 2. Scanning electron microscope images of electropolymerized poly(EDOT−OH) nanostructures by applying a constant voltage (*vs* Ag/Ag$^+$): (a) 1.2 V at 25 °C for 30 s; (b) 1.4 V at 25 °C for 30 s; 1.4 V at 0 °C for (c) 30 s, (d) 60 s, and (e) 90 s. (f) High magnification images of the poly(EDOT−OH) nanostructures in panel c.

at 25 °C. When the applied voltage was increased from 1.2 to 1.4 V (*vs* Ag/Ag$^+$), the density of the nanodots increased under the same electropolymerization time as shown in Figure 2b. More interestingly, poly(EDOT−OH) formed tubular nanostructures when electropolymerization proceeded at 0 °C as shown in Figure 2c−e. When electropolymerization was performed for 30 s, some nanodots were formed on the substrates. When the polymerization time increased to 60 and 90 s, the more obvious and longer tubular structures were observed as shown in Figure 2d,e. Compared to Figure 2b, poly(EDOT−OH) formed totally different nanostructures when electropolymerization was changed from 25 to 0 °C. The effect of temperature on the formation of nanostructures was observed for the PEDOT system shown in Figure 1. From the high resolution as shown in Figure 2f, poly(EDOT−OH) formed clear domains compared to PEDOT as shown in Figure 1f. This indicates that hydroxyl functional groups affect the polymer growth and morphology. Furthermore, this influence is temperature sensitive, which leads to different nanostructures when the electropolymerization was performed at 25 °C compared to at 0 °C. The SEM images of PEDOT and poly(EDOT−OH) prepared at 25 °C by applying different voltages between 1.2 and 1.5 V (*vs* Ag/Ag$^+$) is provided in the Supporting Information. The electropolymerization current−time (*I*−*t*) curves of PEDOT and poly(EDOT−OH) by applying a constant voltage at 1.4 V (*vs* Ag/Ag$^+$) at 0 and 25 °C are also provided in the Supporting Information. By the integration of the current and time, we then calculated the charged cost for the electropolymerization of PEDOT (0.046 C/cm^2), poly(EDOT−OH) (0.086 C/cm^2) at 0 °C for 90 s and PEDOT (0.021 C/cm^2), poly(EDOT−OH) (0.032 C/cm^2) at 25 °C for 30 s. The current was usually steady when 1.4 V (*vs* Ag/Ag$^+$) was applied, although the current of each monomer was different. The current was also slightly influenced by solution temperature. The current was generally higher at 25 °C than at 0 °C, indicating a faster polymerization rate at higher temperature. Other functionalized EDOT and

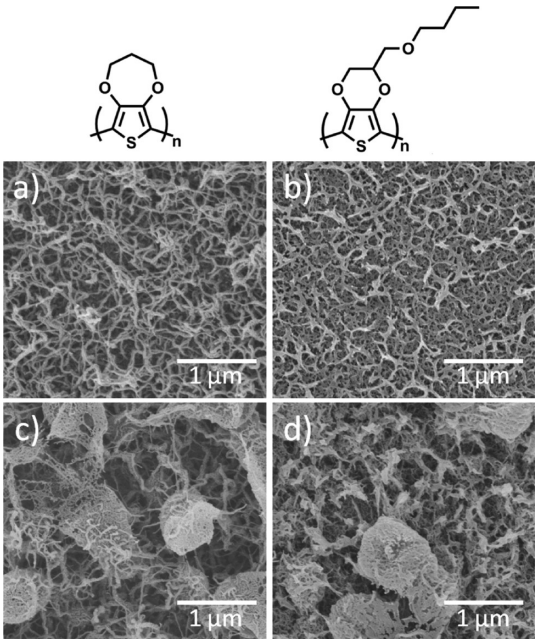

Figure 3. Scanning electron microscope images of electropolymerized (a) poly(ProDOT) and (b) poly(EDOT−C4) by applying a constant voltage of 1.4 V (*vs* Ag/Ag$^+$) at 25 °C for 30 s; electropolymerized (c) poly(ProDOT) and (d) poly(EDOT−C4) by applying a constant voltage of 1.4 V (*vs* Ag/Ag$^+$) at 0 °C for 90 s.

ProDOT structures also showed steady current when 1.4 V (*vs* Ag/Ag$^+$) was applied. Therefore, the electropolymerization by applying a constant voltage at 1.4 V (*vs* Ag/Ag$^+$) was used for making functionalized PEDOT and poly(ProDOT) nanostructures in this research.

After evaluation of the nanostructures of various functional EDOTs and ProDOT prepared by using this template-free electropolymerization in the same solvent system, we then realized the growth mechanism and nanostructures of all tested functionalized EDOTs and ProDOTs were either similar to the PEDOT growth mechanism or the poly(EDOT−OH) growth mechanism. The chemical structures and SEM images of poly(ProDOT) and poly(EDOT−C4) were shown as Figure 3. Similar to EDOT, ProDOT also formed nanofibers when the electropolymerization was performed at 25 °C as shown at Figure 3a. Poly(EDOT−C4) also formed fibrous-type nanostructures as shown in Figure 3b. The nanofibers were not as long and regular as PEDOT or poly(ProDOT) nanofibers, which indicated that the alkyl side chains played an important role for the formation of nanostructures and hindered the regularity when the polymer grew. When poly(ProDOT) and poly(EDOT−C4) were prepared at 0 °C, although nanofibers were formed similar to the nanostructures prepared at 25 °C, some parts of these nanofibers tended to aggregate as shown in Figure 3c,d. The reduction of temperature not only lowered the electropolymerization rate but also caused a slower diffusion rate of monomers, which may be the key factor for this phenomenon. On the other hands, we observed that poly(ProDOT−OH),

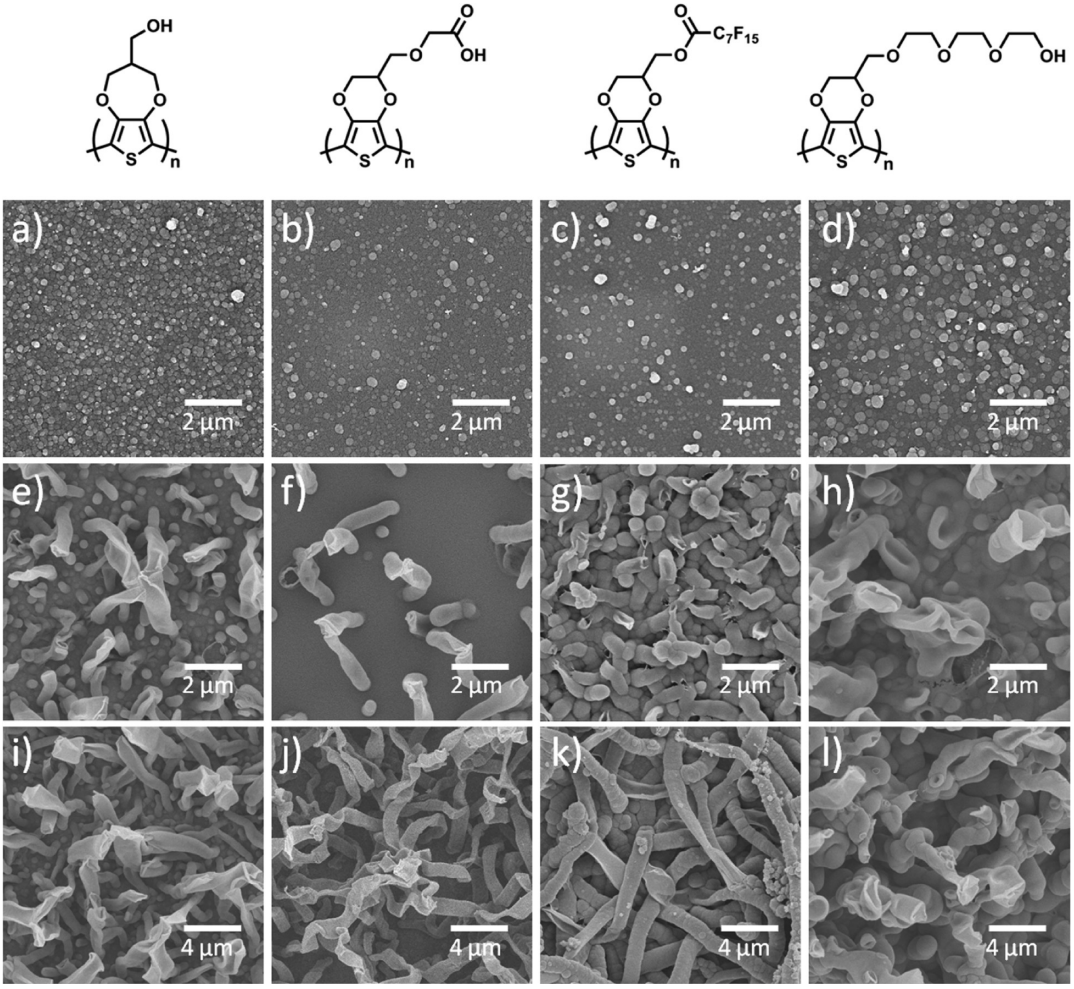

Figure 4. Scanning electron microscope images of electropolymerized (a,e,i) poly(ProDOT−OH), (b,f,j) poly(EDOT−COOH), (c,g,k) poly(EDOT−F), and (d,h,l) poly(EDOT−EG3) by applying a constant voltage of 1.4 V (*vs* Ag/Ag$^+$) at 25 °C for (a−d) 30 s, at 0 °C for (e−h) 90 s, and (i−l) 180 s.

poly(EDOT−COOH), poly(EDOT−EG3), and poly(EDOT−F) formed similar nanostructures, and the temperature effect was similar to poly(EDOT−OH) when the electropolymerization was performed at the same solvent system. As shown in Figure 4a−d, poly(ProDOT−OH), poly(EDOT−COOH), poly(EDOT−EG3), and poly(EDOT−F) all formed nanodots when the electropolymerization was performed at 25 °C. When the electropolymerization was performed at 0 °C, the polymers formed tubular structures as shown in Figure 4e−h. The density and the length of these tubular structures also increased according to electropolymerization as shown in Figure 4i−l. Although the detail of this growth mechanism is still unknown, on the basis of these results, EDOTs or ProDOTs containing polar functional groups tended to form tubular structures when electropolymerization was performed at low temperature. Besides, the shape and length of these tubular structures of different functional groups were different, which indicates the functional groups play a critical role on the formation of tubular structures.

The surface wettibility is governed by both chemical composition and microstructures. More recently, researchers have learned from the nature and understood that superhydrophobic surfaces can be achieved by fine-tuning the nano/micro-structures.[49−51] Here we also evaluated the relationship between surface morphology and wettability by measuring the water contact angle on poly(EDOT−OH), poly(ProDOT−OH), poly(EDOT−COOH), poly(EDOT−EG3), and poly(EDOT−F) of different surface structures as shown in Figure 5. For these five polymers,

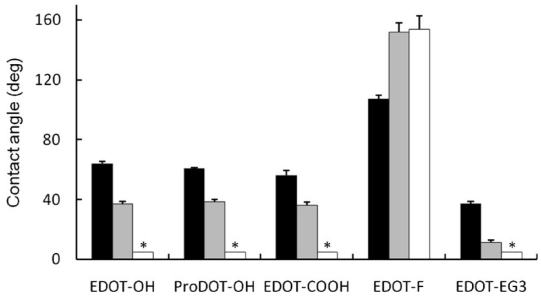

Figure 5. Contact angle measurement of water droplet on poly(EDOT−OH), poly(ProDOT−OH), poly(EDOT−COOH), poly(EDOT−F), and poly(EDOT−EG3) films prepared by applying a constant voltage of 1.4 V (*vs* Ag/Ag$^+$) at 0 °C for 30 s (black), 90 s (gray), and 180 s (white).

TABLE 1. Normalized Cathodal Charge Storage Capacity

polymers	polymerized at 25 °C for 30 s	polymerized at 0 °C for 30 s	polymerized at 0 °C for 90 s
PEDOT	0.104	0.099	0.094
poly(EDOT—OH)	0.089	0.115	0.113
poly(EDOT—COOH)	0.118	0.132	0.133
poly(EDOT—EG3)	0.083	0.096	0.090
poly(EDOT—C4)	0.076	0.070	0.059
poly(EDOT—F)	0.054	0.047	0.010
poly(ProDOT)	0.095	0.088	0.087
poly(ProDOT—OH)	0.085	0.101	0.094

when the films were prepared by applying a constant voltage at 1.4 V for 20 s, the surfaces were generally smooth with some nanodots as shown in Figure 2c. Poly(EDOT—OH) (63.8 deg), poly(ProDOT—OH) (60.5 deg), poly(EDOT—COOH) (56.0 deg), and poly(EDOT—EG3) (36.9 deg) provided hydrophilic surfaces while poly(EDOT—F) (131.9 deg) presented hydrophobic surfaces. When the polymerization time increased to 90 s, the formation of tubular structures (Figure 4e—h) increased the surface roughness, which lead to an enhancement surface wettability. Hydrophilic surfaces became more hydrophilic (poly(EDOT—OH) (37.5 deg), poly(ProDOT—OH) (38.3 deg), poly(EDOT—COOH) (36.15 deg), and poly(EDOT—EG3) (15.4 deg)), while hydrophobic surfaces became more hydrophobic ((poly(EDOT—F) (150.5 deg)). When the polymerization time extended to 180 s, the dense tubular structures were distributed on the surfaces as shown in Figure 4(i—l). For these films, the water drops rapidly spread on all the hydrophilic films (poly(EDOT—OH), poly(ProDOT—OH), poly(EDOT—COOH), and poly(EDOT—EG3), whereas the water was able to slide on the poly(EDOT—F) films.

We also estimated the cathodal charge storage capacity (CSC_c) of these polymer nanostructures which is an important index for neural stimulation electrodes.[52] The CSC_c was calculated from the integral of the cathodic current as shown in the Supporting Information. In this research, we would like to particularly illustrate the functional groups and nanostructure effect on CSC_c. Usually, CSC_c is normalized by the weight of electrode materials. But this kind of normalization is not relevant to this study because each monomer has a different molecular weight. Theoretically, the degree of polymerization using electropolymerization is proportional to the cost charge.[47] Therefore, instead of normalization by film weight, CSC_c was normalized by dividing by the charge cost during the electropolymerization as shown in Table 1. Generally, except for poly(EDOT—F), the normalized CSC_c of individual polymer films prepared by applying 1.4 V (*vs* Ag/Ag^+) for 30 s at 0 °C was quite similar to that of the films prepared by applying 1.4 V (*vs* Ag/Ag^+) for 90 s at 0 °C. This indicates that an increase of deposited polymer amount provides higher electrode capacity. Interestingly, poly(EDOT—F) showed much lower

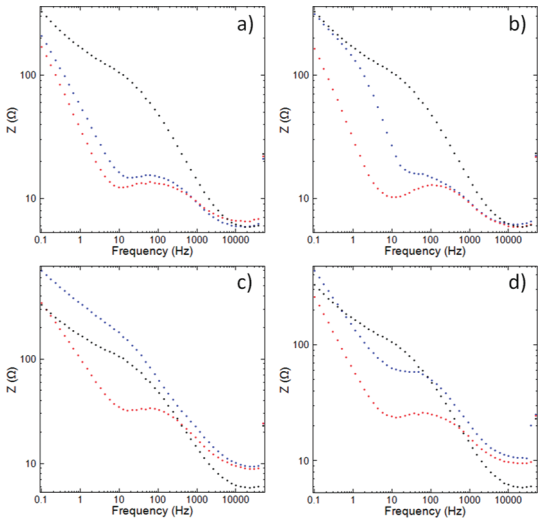

Figure 6. Electrochemical impedance spectroscopy (Bode plots) of (a) PEDOT; (b) poly(EDOT—COOH); (c) poly(EDOT—F); (d) poly(ProDOT—OH). Blue dot line represents the polymer films prepared by applying a constant voltage of 1.4 V (*vs* Ag/Ag^+) at 25 °C for 30 s. Red dot line represents the polymer films prepared by applying a constant voltage of 1.4 V (*vs* Ag/Ag^+) at 0 °C for 90 s. Au surface (black dot line) is used as a comparison.

normalized CSC_c when the polymer films become thicker, which may be due to the superhydrophobic surface properties. On the other hand, poly(EDOT—COOH), which has the only ionic functional group among the test polymers, showed the highest normalized CSC_c for polymer films regardless of film preparation methods. Although the normalized CSC_c was different in a comparison of the films prepared from 0 °C to those prepared from 25 °C, the difference was not as clear as the difference caused by different polymers. This indicates that the functionalized group effect is more dominant on the normalized CSC_c compared to structure effect.

Martin's group pioneered the use of conducting polymers for neuron probes and has successfully demonstrated that PEDOT-based electrodes provide lower impedance compared to bare Au electrodes.[13] Here, we also evaluated the impedance of representative functionalized PEDOT-coated electrodes as shown in Figure 6. In Figure 6a, the impedance of PEDOT electrodes prepared at both 25 and 0 °C were much lower than bare Au electrode when the frequency is lower than 100 Hz. This is mainly due to an increase in effective surface area of the electrode[13] which is provided by the PEDOT nanowires and nanonetworks. The similar impedance between PEDOT prepared at 25 and 0 °C indicated the similar effective surfaces between nanowires and nanonetwork structures. Different from PEDOT electrodes, poly(EDOT—COOH) (Figure 6b), poly(EDOT—F) (Figure 6c), and poly(ProDOT) (Figure 6d) prepared at 25 °C showed higher impedance compared to films prepared at 0 °C when the frequency is lower than 100 Hz. This indicated the tubular structures prepared at 0 °C provided more

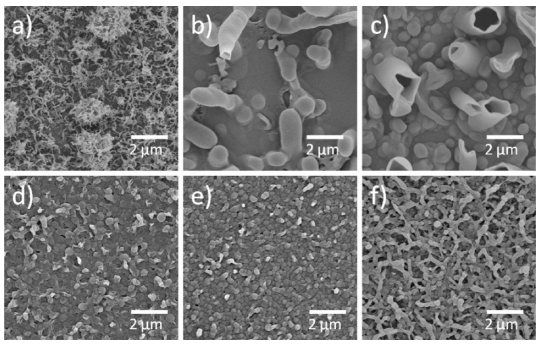

Figure 7. The SEM measurement of copolymer films prepared from mixed monomer solutions of (a) [EDOT] = 7.5 mM and [EDOT−OH] = 2.5 mM; (b) [EDOT] = 5 mM and [EDOT−OH] = 5 mM; (c) [EDOT] = 2.5 mM and [EDOT−OH] = 7.5 mM; (d) [EDOT−EG3] = 7.5 mM and [EDOT−F] = 2.5 mM; (e) [EDOT−EG3] = 5 mM and [EDOT−F] = 5 mM; (f) [EDOT−EG3] = 2.5 mM and [EDOT−F] = 7.5 mM. Films were prepared by applying a constant voltage of 1.4 V (*vs* Ag/Ag$^+$) at 0 °C for 60 s.

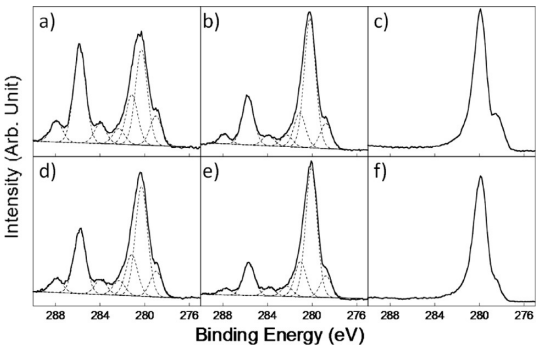

Figure 8. The XPS measurement of poly(EDOT−F)-*co*-(EDOT−EG3) films prepared from monomer solution of (a and d) [EDOT−F] = 7.5 mM; [EDOT−EG3] = 2.5 mM; (b and e) [EDOT−F] = 5 mM; [EDOT−EG3] = 5 mM; (c and f) [EDOT−F] = 2.5 mM; [EDOT−EG3] = 7.5 mM. For (a,b,c), films prepared by applying a constant voltage of 1.4 V (*vs* Ag/Ag$^+$) at 0 °C for 30 s; for (d,e,f), films prepared by applying a constant voltage of 1.4 V (*vs* Ag/Ag$^+$) at 0 °C for 60 s.

effective surface area compared to nanodot structures prepared at 25 °C. In a comparison of the impedance of these three functionalized polymers, poly(EDOT−F) showed the highest impedance in general, whereas poly(EDOT−COOH) provided similar impedance as PEDOT. The impedance of poly(EDOT−F) prepared at 25 °C was even higher than Au. This indicated that impedance is also influenced by functional groups.

Although we have demonstrated our interesting finding on creating various functionalized PEDOT nanostructures by a template-free electropolymerization method, we also want to discuss the restriction and limitation of using this method to make PEDOT nanostructures. One important advantage of using electropolymerization to prepare polymer films is the flexibility to tune the film properties by simply mixing two or more than two different monomers during the electropolymerization. Previous we already demonstrated that regular nanostructures can be achieved for homopolymers. Therefore, it is quite interesting to know how the nanostructures change when a copolymerization is performed. Here we explored two copolymer systems, poly(EDOT-*co*-EDOT−OH) and poly(EDOT−EG3-*co*-EDOT−F), prepared at 0 °C as shown in Figure 7. The nanostructures of poly(EDOT-*co*-EDOT−OH) in different chemical compositions were shown in Figure 7a−c. PEDOT and poly(EDOT−OH) homopolymers formed different nanostructures, that is, PEDOT formed nanowires while poly(EDOT−OH) formed tubular structures when the electropolymerization was performed at 0 °C. As shown in Figure 7a, when the monomer concentration of EDOT−OH is only 25%, the copolymers formed nanofiber-like structures, which indicates EDOT dominated the formation of nanostructures. When the monomer concentration of EDOT−OH was increase to 50%, some nanostructures that looked like tubular structures were formed. After the monomer concentration was increased to 75%, the large and obvious tubular structures were observed. Although the nanostructure may not be as regular as homopolymers, for poly(EDOT-*co*-EDOT−OH), the general tendency of nanostructure formation can still be predicted by the composition of monomer solutions. Second, we evaluated the copolymers of poly(EDOT−EG3-*co*-EDOT−F). We have demonstrated these two polymers both formed tubular structures when electropolymerization was performed at 0 °C. For copolymers, however, when the monomer concentration of EDOT−EG3 was 75% and 50%, no obvious tubular structures were observed as shown in Figure 7d and Figure 7e. Only when the concentration of EDOT−F was increased to 75% were more organized tubular structures observed as shown in Figure 7f. Although we did not screen all the combination of copolymers and their nanostructures, the results of these two examples, poly(EDOT-*co*-EDOT−OH) and poly(EDOT−F-*co*-EDOT−EG3), illustrated the irregularity and unpredictability of the nanostructures of the copolymers due to the complex interaction between different functional groups.

Besides the irregularity and unpredicted nanostructures for copolymers, the changing of chemical composition during the electropolymerization is another important issue to be pointed out here. We evaluated the chemical compositions of the copolymer, poly(EDOT−F-*co*-EDOT−EG3), by using XPS as shown in Figure 8. The high binding energy C1s peaks between 284 to 288 eV indicated the perfluorocarbon. The ratio of perfluorocarbon peak was decreased when the EDOT−F monomer concentration was decreased as shown in Figure 8a−c, which indicated the composition of EDOT−F in the copolymers decreased. Furthermore, in a comparison of Figure 8d,e to Figure 8a,b, when the electropolymerization time was increased from 30 to 60 s, the ratio of EDOT−F also decreased. That indicated the polymerization rate of EDOT−F was

slower than EDOT−EG3, which leads to lower composition when the polymerization time was longer. In fact, when the concentration of EDOT−F was lowered to 25%, the high binding energy C1s peaks already could not be observed even with shorter electropolymerization time as shown in Figure 8c. It also indicated a slower polymerization of EDOT−F compared to EDOT−EG3. Therefore, to accurately control the chemical composition of copolymers, not only the concentration of monomer solutions but also the electropolymerization time needs to be managed carefully.

CONCLUSIONS

In this work, we have demonstrated the influence of functional groups on the formation of PEDOT and poly(ProDOT) nanostructures. For unfunctionalized EDOT, ProDOT, and EDOT with nonpolar functional groups such as alkyl chains, the polymers formed nanofibers and nanoporous structures in general. On the other hand, for EDOT and ProDOT containing polar functional groups, such as hydroxyl, carboxylic acid, triethylene glycol, and perfluorocarbon, the polymers formed nanodots when electropolymerized at 25 °C, while they formed tubular structures when electropolymerized at 0 °C. By water contact angle measurement, the surface wettability and hydrophobicity were enhanced when the nanostructures were formed. From the normalized CSC_c results, poly(EDOT−COOH) films provided the highest capacity, whereas poly(EDOT−F) showed the lowest capacity when the same charge was applied for electropolymerization. For the EIS measurement, except poly(EDOT−F) films of nanodot structure, the impedance of functionalized PEDOT films were generally lower than Au when the frequency was lower than 100 Hz mainly due to an increase in effective surface area of PEDOT electrodes. Similar to CSC_c results, the functional group also played an important role on impedance. We further evaluated the nanostructures prepared from the copolymerization of several different functionalized EDOTs. Unpredictable and fairly organized nanostructures were observed mainly due to the complex interaction between different functionalized EDOTs during electropolymerization. On the basis of these results, various conducting polymer nanostructures can also be created directly by using electropolymerization without templates when the environmental parameters are carefully controlled. Although a template-free method is straightforward and convenient, for copolymer systems, to control the compositions and nanostructures is quite challenging. It may be the main restriction of this method.

EXPERIMENTAL SECTION

Monomer Synthesis. 3,4-ethylenedioxythiophene (EDOT), hydroxymethyl EDOT (EDOT−OH), and 3,4-propylenedioxythiophene (ProDOT) were purchased from Sigma-Aldrich. The EDOT−COOH,[38] EDOT−F,[53] EDOT−C4,[54,55] and ProDOT−OH[56] were synthesized by following previous publications. Shortly, for EDOT−COOH, a 100 mL round-bottom flask was charged with a stir bar, EDOT−OH (861 mg, 5.0 mmol), NaI (150 mg, 1.0 mmol), and NaH (60% suspension in mineral oil, 240 mg, 6.0 mmol), and the flask was backfilled with argon. Dry tetrahydrofuran (THF; 20 mL) was introduced, and the suspension was stirred for 15 min and cooled in an ice bath. Methyl bromoacetate (0.57 mL, 0.92 g, 6.0 mmol) was added dropwise, and the reaction mixture was stirred for 18 h. The majority of THF was removed with a rotary evaporator; the crude product was partitioned between water and ethyl acetate, and the aqueous layer was extracted with ethyl acetate. The combined organic layers were washed with brine, dried ($MgSO_4$), and evaporated. After purification with a silica gel column (hexane/ethyl acetate =5:1), the product (610 mg) was dissolved in THF (10 mL) in a 100 mL round-bottom flask, and freshly prepared aqueous NaOH solution (2 M, 10 mL) was added. The mixture was stirred vigorously until the starting material was completely consumed by thin layer chromatography. The mixture was acidified to pH < 3 and then extracted with ethyl acetate. The combined organic layers were washed with water, dried ($MgSO_4$), and evaporated. EDOT−COOH (480 mg, 63%) was obtained. ^{1}H NMR ($CDCl_3$): δ 6.36 (d, 2H, J = 3.6 Hz), 6.34 (d, 1H, J = 3.6 Hz), 4.38 (ddd, 1H, J = 11.6, 7.2, 2.4 Hz), 4.26 (dd, 1H, J = 11.6, 2.4 Hz), 4.24 (s, 2H), 4.12 (dd, 1H, J = 11.6, 7.2 Hz), 3.85 (dd, 1H, J = 10.4, 4.8 Hz), 3.81 (dd, 1H, J = 10.4, 4.8 Hz). ^{13}C NMR ($CDCl_3$): δ 175.2, 141.3, 141.1, 100.0, 99.9, 72.6, 70.0, 68.4, 65.8. HRMS (FAB): [M + H] calcd for $C_9H_{11}O_5S$, 231.0237; found, 231.0237. For EDOT−F, a 300 mL round-bottom flask was charged with a stir bar, EDOT−OH (500 mg, 2.9 mmol), CH_2Cl_2 (20 mL), and triethylamine (310 mg, 3.1 mmol), and the flask was backfilled with argon. A solution of CH_2Cl_2 (20 mL) and perfluoro acid chloride (1.35 g, 3.13 mmol) was added slowly. The solution was continuously stirred for 2 h before it was poured into 100 mL of 1 M HCl. The organic layer was washed with concentrated $NaHCO_3$ followed by brine. After it was dried over $MgSO_4$, the crude product was purified by column chromatography to yield a white powder (0.76 g, 46%). ^{1}H NMR ($CDCl_3$): δ 6.36 (d, 2H, J = 3.7), 4.57 (m, 2H), 4.46 (m, 1H), 4.22 (dd, 1H, J = 11.7, 2.4 Hz), 4.06 (dd, 1H, J = 11.7, 6.3 Hz), 3.85 (dd, 1H, J = 10.4, 4.8 Hz). ^{13}C NMR ($CDCl_3$): δ 158.0, 140.8, 140.3, 100.6, 100.4, 70.4, 65.5, 64.8. ^{19}F NMR ($CDCl_3$): δ −126.2, 122.8, −122.6, −122.0, −121.7, −118.4 (CF_2−CO), −80.8 (CF_3). HRMS: calcd for $C_{15}H_7F_{15}O_4S$, 567.9825; found, 567.9823. For EDOT−C4, a 100 mL round-bottom flask was charged with a stir bar, EDOT−OH (1 g, 5.80 mmol), 18-Crown-6 (154 mg, 0.58 mmol), and NaH (60% suspension in mineral oil, 1.16 g, 29.0 mmol), and the flask was backfilled with argon. Dry THF (40 mL) was introduced, and the suspension was stirred for 15 min and cooled in an ice bath. 1-Bromobutane (0.75 mL, 0.96 g, 6.9 mmol) was added dropwise, and the reaction mixture was stirred for 18 h. The majority of THF was removed with a rotary evaporator; the crude product was partitioned between water and ethyl acetate, and the aqueous layer was extracted with ethyl acetate. The combined organic layers were washed with brine, dried ($MgSO_4$), and evaporated. After purification with a silica gel column (hexane/ethyl acetate = 20:1), the product (1.14 g, 86%) was received. ^{1}H NMR ($CDCl_3$): δ 6.31 (d, 2H, J = 3.7), 4.28 (m, 1H), 4.22 (dd, 1H, J = 11.6, 2.2 Hz), 4.03 (dd, 1H, J = 11.7, 7.6 Hz), 1.55 (m, 2H), 1.35 (m, 2H). 0.9 (t, 3H, J = 7.4), ^{13}C NMR ($CDCl_3$): δ 141.6, 141.6, 99.7, 99.5, 72.6, 71.8, 69.1, 66.2. 31.6, 19.2, 13.9. HRMS (EI): calcd for $C_{11}H_{16}O_3S$, 228.0820; found, 228.0818. For ProDOT−OH, to a mixture of 3,4-dimethoxythiophene (1 g, 7.0 mmol) and 1,1,1-tris(hydroxymethyl)methane

(880 mg, 8.3 mmol) dissolved in 200 mL of dry toluene was added a catalytic amount of *p*-toluene sulfonic acid, and the mixture was refluxed for 16 h over a molecular sieve (4 Å). The majority of toluene was removed with a rotary evaporator, and the residue was taken up in CH_2Cl_2. The resulting solution was subsequently extracted with water, and the organic layer was dried over $CaCl_2$ and concentrated. The crude product was purified by column chromatography (hexane/CH_2Cl_2 = 1:1) to yield the final product (625 mg, 48%). ^{1}H NMR ($CDCl_3$): δ 6.47 (s, 2H), 4.15 (dd, 2H, J = 12.2, 5.4 Hz), 4.08 (dd, 2H, J = 12.3, 3.4 Hz), 2.30 (m, 1H), 2.22 (s, 2H). ^{13}C NMR ($CDCl_3$): δ 149.9, 106.0, 71.9, 60.7, 44.9. HRMS (EI): calcd for $C_8H_{10}O_3S$, 186.0351; found, 186.0350. EDOT−EG3 was prepared by the following synthesis steps. Trityl chloride (5.58 g) was dissolved in a mixture of triethylene glycol (13.3 mL) and dichloromethane (25 mL). After pyridine (1.6 mL) was added, the mixture was stirred overnight, then diluted with dichloromethane and washed with H_2O. To the solution, a stir bar and triethylamine (4 mL) was added, the flask was cooled at 0 °C, and MsCl (2.3 mL) was added dropwise. After being stirred overnight, the solution was quenched with H_2O (5 min stirring), washed with saturated $NaHCO_3$, dried over $MgSO_4$, and purified by chromatography. In a 250 mL flask EDOT−OH (5.41 g), NaI (0.471 g), and a stirrer were sealed and backfilled with N_2. Dried DMF (40 mL) and 1.88 g of NaH were added under N_2 flow. The reaction was stirred for 15 min, a solution of 14.79 g product in DMF (30 mL) was added, and the mixture was stirred overnight, then dissolved in 200 mL of EA, and washed with H_2O. The solvent was removed by a rotavapor and the residue was dispersed in methanol (400 mL) with Amberlite (40 g). After being stirred at 70 °C and refluxed over 6 h, the resin was filtered and purified by chromatography. ^{1}H NMR ($CDCl_3$): δ 6.33 (s, 2H), 4.34 (m, 1H), 4.26 (dd, J = 11.6, 2.4 Hz, 1H), 4.07 (dd, J = 11.6, 7.6 Hz, 1H), 3.79−3.66 (m, 12H), 3.61 (m, 2H), 2.42 (broad s, 1H). ^{13}C NMR ($CDCl_3$): δ 141.5, 141.4, 99.7, 99.6, 72.6, 72.5, 71.1, 70.7, 70.5, 70.3, 69.6, 66.1, 61.7. HRMS (FAB): calcd for $C_{13}H_{21}O_6S$ ($[M+H]^+$), 305.1059; found, 305.1050. The chemicals for synthesis were purchased from Sigma-Aldrich and Tokyo Chemical Industry Co. Ltd.

Electropolymerization. Monomer solutions were prepared by dissolving monomers at a concentration of 10 mM in dichloromethane containing 100 mM tetrabutyl ammonium perchlorate as electrolyte. The solutions were stabilized at controlled temperature for 3 min to reach equilibrium before performing electropolymerization. The electropolymerization was performed by using a potentiostat (PGSTAT128N, Autolab) with a Ag/Ag^+ electrode (RE-7, BAS) as reference electrode, and a Pt wire as counter-electrode. Nanostructured PEDOTs were mainly fabricated by electropolymerization using a constant voltage method.

Electrochemical Properties Characterization. For the estimation of cathodal charge storage capacity (CSC_c), polymer films were deposited on ITO-coated glass of 1 cm^2 area. The cyclic voltammetry was performed in PBS buffer at scanning rate of 50 mV sec^{-1} from −0.6 to 0.6 V. The normalized (CSC_c) was obtained by dividing the original CSC_c value to the charge consumed during electropolymerization. The electrochemical impedance spectroscopy (EIS) measurements were performed in PBS buffer in the presence of 10 mM $[Fe(CN)_6]^{3-/4-}$ (1:1 mol/mol) as redox couple at 25 °C. The measurement was performed with 10 mV sinusoidal modulation amplitude in the frequency range of 0.1 Hz to 50 kHz at 50 steps upon biasing the working electrode at 0.2 V *vs* Ag/AgCl.

Surface Characterization. SEM was conducted by a FE-SEM (JSM-6330F, JEOL). A thin layer Au (<3 nm) was coated on samples for SEM experiments. X-ray photoelectron spectroscopy (XPS) was conducted by an ESCALAB 250 (Thermo VG) system. Contact angle was measured by using a contact angle measurement system (SImage mini, Excimer, Inc.)

Conflict of Interest: The authors declare no competing financial interest.

Acknowledgment. This work was financially supported by RIKEN Advanced Science Institute and Grant-in-Aid for Young Scientist (No. 22681016 and 23710138) from JSPS/MEXT, Japan.

Supporting Information Available: Additional explanations and graphics as described in the text. This material is available free of charge *via* the Internet at http://pubs.acs.org.

REFERENCES AND NOTES

1. Li, C.; Bai, H.; Shi, G. Q. Conducting Polymer Nanomaterials: Electrosynthesis and Applications. *Chem. Soc. Rev.* **2009**, *38*, 2397–2409.
2. Li, D.; Huang, J. X.; Kaner, R. B. Polyaniline Nanofibers: A Unique Polymer Nanostructure for Versatile Applications. *Acc. Chem. Res.* **2009**, *42*, 135–145.
3. Tran, H. D.; Li, D.; Kaner, R. B. One-Dimensional Conducting Polymer Nanostructures: Bulk Synthesis and Applications. *Adv. Mater.* **2009**, *21*, 1487–1499.
4. Cao, Y.; Kovalev, A. E.; Xiao, R.; Kim, J.; Mayer, T. S.; Mallouk, T. E. Electrical Transport and Chemical Sensing Properties of Individual Conducting Polymer Nanowires. *Nano Lett.* **2008**, *8*, 4653–4658.
5. Lee, J. I.; Cho, S. H.; Park, S.-M.; Kim, J. K.; Kim, J. K.; Yu, J.-W.; Kim, Y. C.; Russell, T. P. Highly Aligned Ultrahigh Density Arrays of Conducting Polymer Nanorods Using Block Copolymer Templates. *Nano Lett.* **2008**, *8*, 2315–2320.
6. Hangarter, C. M.; Bangar, M.; Mulchandani, A.; Myung, N. V. Conducting Polymer Nanowires for Chemiresistive and FET-Based Bio/Chemical Sensors. *J. Mater. Chem.* **2010**, *20*, 3131–3140.
7. Ramgir, N. S.; Yang, Y.; Zacharias, M. Nanowire-Based Sensors. *Small* **2010**, *6*, 1705–1722.
8. Ghosh, S.; Inganäs, O. Conducting Polymer Hydrogels as 3D Electrodes: Applications for Supercapacitors. *Adv. Mater.* **1999**, *11*, 1214–1218.
9. Liu, R.; Duay, J.; Lee, S. B. Redox Exchange Induced MnO_2 Nanoparticle Enrichment in Poly(3,4-ethylenedioxythiophene) Nanowires for Electrochemical Energy Storage. *ACS Nano* **2010**, *4*, 4299–4307.
10. Winther-Jensen, B.; Winther-Jensen, O.; Forsyth, M.; MacFarlane, D. R. High Rates of Oxygen Reduction Over a Vapor Phase-Polymerized PEDOT Electrode. *Science* **2008**, *321*, 671–674.
11. Garner, B.; Georgevich, A.; Hodgson, A. J.; Liu, L.; Wallace, G. G. Polypyrrole-Heparin Composites as Stimulus-Responsive Substrates for Endothelial Cell Growth. *J. Biomed. Mater. Res.* **1999**, *44*, 121–129.
12. Kim, D. H.; Abidian, M.; Martin, D. C. Conducting Polymers Grown in Hydrogel Scaffolds Coated on Neural Prosthetic Devices. *J. Biomed. Mater. Res. Part A* **2004**, *71A*, 577–585.
13. Richardson-Burns, S. M.; Hendricks, J. L.; Foster, B.; Povlich, L. K.; Kim, D. H.; Martin, D. C. Poly(3,4-ethylenedioxythiophene) as a Micro-neural Interface Material for Electrostimulation. *Biomaterials* **2007**, *28*, 1539–1552.
14. Berggren, M.; Richter-Dahlfors, A. Organic Bioelectronics. *Adv. Mater.* **2007**, *19*, 3201–3213.
15. Yoon, H.; Ko, S.; Jang, J. Field-Effect-Transistor Sensor Based on Enzyme-Functionalized Polypyrrole Nanotubes for Glucose Detection. *J. Phys. Chem. B* **2008**, *112*, 9992–9997.
16. Owens, R. M.; Malliaras, G. G. Organic Electronics at the Interface with Biology. *MRS Bull.* **2010**, *35*, 449–456.
17. Luo, S. C.; Xie, H.; Chen, N. Y.; Yu, H. H. Trinity DNA Detection Platform by Ultrasmooth and Functionalized PEDOT Biointerfaces. *ACS Appl. Mater. Interfaces* **2009**, *1*, 1414–1419.
18. Peng, H.; Soeller, C.; Travas-Sejdic, J. Novel Conducting Polymers for DNA Sensing. *Macromolecules* **2007**, *40*, 909–914.
19. Thompson, B. C.; Richardson, R. T.; Moulton, S. E.; Evans, A. J.; O'Leary, S.; Clark, G. M.; Wallace, G. G. Conducting Polymers, Dual Neurotrophins and Pulsed Electrical Stimulation—Dramatic Effects on Neurite Outgrowth. *J. Controlled Release* **2010**, *141*, 161–167.
20. Martin, D. C.; Wu, J. H.; Shaw, C. M.; King, Z.; Spanninga, S. A.; Richardson-Burns, S.; Hendricks, J.; Yang, J. Y. The Morphology of Poly(3,4-ethylenedioxythiophene). *Polym. Rev.* **2010**, *50*, 340–384.

21. Simon, D. T.; Kurup, S.; Larsson, K. C.; Hori, R.; Tybrandt, K.; Goiny, M.; Jager, E. H.; Berggren, M.; Canlon, B.; Richter-Dahlfors, A. Organic Electronics for Precise Delivery of Neurotransmitters to Modulate Mammalian Sensory Function. *Nat. Mater.* **2009**, *8*, 742–746.
22. Guimard, N. K.; Gomez, N.; Schmidt, C. E. Conducting Polymers in Biomedical Engineering. *Prog. Polym. Sci.* **2007**, *32*, 876–921.
23. Asplund, M.; Nyberg, T.; Inganäs, O. Electroactive Polymers for Neural Interfaces. *Polym. Chem.* **2010**, *1*, 1374–1391.
24. Asplund, M.; Thaning, E.; Lundberg, J.; Sandberg-Nordqvist, A. C.; Kostyszyn, B.; Inganäs, O.; von Holst, H. Toxicity Evaluation of PEDOT/Biomolecular Composites Intended for Neural Communication Electrodes. *Biomed. Mater.* **2009**, *4*, 045009.
25. Lock, J. P.; Im, S. G.; Gleason, K. K. Oxidative Chemical Vapor Deposition of Electrically Conducting Poly(3,4-ethylenedioxythiophene) Films. *Macromolecules* **2006**, *39*, 5326–5329.
26. Luo, S. C.; Jiang, J.; Liour, S. S.; Gao, S. J.; Ying, J. Y.; Yu, H. H. Magnetic PEDOT Hollow Capsules with Single Holes. *Chem. Commun.* **2009**, 2664–2666.
27. Luo, S. C.; Yu, H. H.; Wan, A. C. A.; Han, Y.; Ying, J. Y. A General Route for Functional PEDOT Coating on Non-conductive Surface and Hollow Particles with Single Hole *via* Aqueous Chemical Polymerization. *Small* **2008**, *4*, 2051–2058.
28. Yoon, H.; Chang, M.; Jang, J. Formation of 1D Poly(3,4-ethylenedioxythiophene) Nanomaterials in Reverse Microemulsions and Their Application to Chemical Sensors. *Adv. Funct. Mater.* **2007**, *17*, 431–436.
29. Reddy, K. R.; Jeong, H. M.; Lee, Y.; Raghu, A. V. Synthesis of MWCNTs-Core/Thiophene Polymer-Sheath Composite Nanocables by a Cationic Surfactant-Assisted Chemical Oxidative Polymerization and Their Structural Properties. *J. Polym. Sci., Part A: Polym. Chem.* **2010**, *48*, 1477–1484.
30. Tran, H. D.; Wang, Y.; D'Arcy, J. M.; Kaner, R. B. Toward an Understanding of the Formation of Conducting Polymer Nanofibers. *ACS Nano* **2008**, *2*, 1841–1848.
31. Xiao, R.; Il Cho, S.; Liu, R.; Lee, S. B. Controlled Electrochemical Synthesis of Conductive Polymer Nanotube Structures. *J. Am. Chem. Soc.* **2007**, *129*, 4483–4489.
32. Il Cho, S.; Lee, S. B. Fast Electrochemistry of Conductive Polymer Nanotubes: Synthesis, Mechanism, and Application. *Acc. Chem. Res.* **2008**, *41*, 699–707.
33. Trujillo, N. J.; Barr, M. C.; Im, S. G.; Gleason, K. K. Oxidative Chemical Vapor Deposition (oCVD) of Patterned and Functional Grafted Conducting Polymer Nanostructures. *J. Mater. Chem.* **2010**, *20*, 3968–3972.
34. Liang, L.; Liu, J.; Windisch, C. F.; Exarhos, G. J.; Lin, Y. H. Direct Assembly of Large Arrays of Oriented Conducting Polymer Nanowires. *Angew. Chem., Int. Ed.* **2002**, *41*, 3665–3668.
35. Luo, S. C.; Liour, S. S.; Yu, H. H. Perfluoro-Functionalized PEDOT Films with Controlled Morphology as Superhydrophobic Coatings and Biointerfaces with Enhanced Cell Adhesion. *Chem. Commun.* **2010**, *46*, 4731–4733.
36. Groenendaal, B. L.; Jonas, F.; Freitag, D.; Pielartzik, H.; Reynolds, J. R. Poly(3,4-ethylenedioxythiophene) and Its Derivatives: Past, Present and Future. *Adv. Mater.* **2000**, *12*, 481–494.
37. Groenendaal, L.; Zotti, G.; Aubert, P. H.; Waybright, S. M.; Reynolds, J. R. Electrochemistry of Poly(3,4-alkylenedioxythiophene) Derivatives. *Adv. Mater.* **2003**, *15*, 855–879.
38. Luo, S. C.; Ali, E. M.; Tansil, N. C.; Yu, H. H.; Gao, S.; Kantchev, E. A. B.; Ying, J. Y. Poly(3,4-ethylenedioxythiophene) (PEDOT) Nanobiointerfaces: Thin, Ultrasmooth, and Functionalized PEDOT Films with *in Vitro* and *in Vivo* Biocompatibility. *Langmuir* **2008**, *24*, 8071–8077.
39. Daugaard, A. E.; Hvilsted, S.; Hansen, T. S.; Larsen, N. B. Conductive Polymer Functionalization by Click Chemistry. *Macromolecules* **2008**, *41*, 4321–4327.
40. Hansen, T. S.; Daugaard, A. E.; Hvilsted, S.; Larsen, N. B. Spatially Selective Functionalization of Conducting Polymers by "Electroclick" Chemistry. *Adv. Mater.* **2009**, *21*, 4483–4486.
41. Lind, J. U.; Hansen, T. S.; Daugaard, A. E.; Hvilsted, S.; Andresen, T. L.; Larsen, N. B. Solvent Composition Directing Click-Functionalization at the Surface or in the Bulk of Azide-Modified PEDOT. *Macromolecules* **2011**, *44*, 495–501.
42. Darmanin, T.; de Givenchy, E. T.; Amigoni, S.; Guittard, F. Hydrocarbon *versus* Fluorocarbon in the Electrodeposition of Superhydrophobic Polymer Films. *Langmuir* **2010**, *26*, 17596–17602.
43. Poverenov, E.; Li, M.; Bitler, A.; Bendikov, M. Major Effect of Electropolymerization Solvent on Morphology and Electrochromic Properties of PEDOT Films. *Chem. Mater.* **2010**, *22*, 4019–4025.
44. Zhou, C. F.; Liu, Z. W.; Du, X. S.; Ringer, S. P. Electro-synthesis of Novel Nanostructured PEDOT Films and Their Application as Catalyst Support. *Synth. Met.* **2010**, *160*, 1636–1641.
45. Wang, X. J.; Sjoberg-Eerola, P.; Eriksson, J. E.; Bobacka, J.; Bergelin, M. The Effect of Counter Ions and Substrate Material on the Growth and Morphology of Poly(3,4-ethylenedioxythiophene) Films: Towards the Application of Enzyme Electrode Construction in Biofuel Cells. *Synth. Met.* **2010**, *160*, 1373–1381.
46. Darmanin, T.; Guittard, F. Superhydrophobic Fiber Mats by Electrodeposition of Fluorinated Poly(3,4-ethyleneoxythiathiophene). *J. Am. Chem. Soc.* **2011**, *133*, 15627–15634.
47. Sadki, S.; Schottland, P.; Brodie, N.; Sabouraud, G. The Mechanisms of Pyrrole Electropolymerization. *Chem. Soc. Rev.* **2000**, *29*, 283–293.
48. Heinze, J.; Frontana-Uribe, B. A.; Ludwigs, S. Electrochemistry of Conducting Polymers-Persistent Models and New Concepts. *Chem. Rev.* **2010**, *110*, 4724–4771.
49. Jiang, L.; Zhao, Y.; Zhai, J. A Lotus-Leaf-like Superhydrophobic Surface: A Porous Microsphere/Nanofiber Composite Film Prepared by Electrohydrodynamics. *Angew. Chem., Int. Ed.* **2004**, *43*, 4338–4341.
50. Feng, L.; Li, S.; Li, Y.; Li, H.; Zhang, L.; Zhai, J.; Song, Y.; Liu, B.; Jiang, L.; Zhu, D. Super-hydrophobic Surfaces: From Natural to Artificial. *Adv. Mater.* **2002**, *14*, 1857–1860.
51. Sun, T.; Feng, L.; Guo, X.; Jiang, L. Bioinspired Surfaces with Special Wettability. *Acc. Chem. Res.* **2005**, *38*, 644–652.
52. Cogan, S. F. Neural Stimulation and Recording Electrodes. *Annu. Rev. Biomed. Eng.* **2008**, *10*, 275–309.
53. Schwendeman, I.; Gaupp, C. L.; Hancock, J. M.; Groenendaal, L.; Reynolds, J. R. Perfluoroalkanoate-Substituted PEDOT for Electrochromic Device Applications. *Adv. Funct. Mater.* **2003**, *13*, 541–547.
54. Czardybon, A.; Lapkowski, M. Synthesis and Electropolymerisation of 3,4-Ethylenedioxythiophene Functionalised with Alkoxy Groups. *Synth. Met.* **2001**, *119*, 161–162.
55. Schottland, P.; Fichet, O.; Teyssié, D.; Chevrot, C. Langmuir–Blodgett Films of an Alkoxy Derivative of Poly(3,4-ethylenedioxythiophene). *Synth. Met.* **1999**, *101*, 7–8.
56. Kros, A.; Nolte, R. J. M.; Sommerdijk, N. Poly(3,4-ethylenedioxythiophene)-Based Copolymers for Biosensor Applications. *J. Polym. Sci., Polym. Chem.* **2002**, *40*, 738–747.